


ORIGINAL RESEARCH

Influence of altitude on tropical marine habitat classification using imagery from fixed-wing, water-landing UAVs

Sophia L. Ellis^{1,2} , Michelle L. Taylor¹, Melissa Schiele^{2,3} & Tom B. Letessier²¹School of Life Sciences, University of Essex, Colchester, United Kingdom²Institute of Zoology, Zoological Society of London, Regent's Park, London, United Kingdom³Wolfson School of Mechanical, Electrical and Manufacturing Engineering, Loughborough University, Leicestershire, United Kingdom

Keywords

Coral, habitat maps, seagrass, tropical marine environments, unmanned aerial vehicles, very high-resolution

Correspondence

Sophia L. Ellis, School of Life Sciences, University of Essex, Colchester, United Kingdom. Tel: 07402213145; E-mail: sophiae941@gmail.com

Editor: Ned Horning

Associate Editor: Dimitris Poursanidis

Received: 9 December 2019; Revised: 2 March 2020; Accepted: 27 March 2020

doi: 10.1002/rse2.160

Abstract

Unmanned aerial vehicles (UAVs) are cost-effective remote sensing tools useful for generating very high-resolution (VHR) aerial imagery. Habitat maps generated from UAV imagery are a fundamental component of marine spatial planning, essential for the designation and governance of marine protected areas (MPAs). We investigated whether UAV survey altitude affects habitat classification performance and the classification accuracy of thematic maps from a tropical shallow water environment. We conducted repeated UAV flights at 75, 85, and 110 m, using a fixed-wing UAV on the Turneffe Atoll, Belize. Flights were ground truthed with snorkel surveys. Images were mosaiced to form orthomosaics and transformed into thematic maps through semi-automatic object-based image analysis (OBIA). Three subset areas (4000 m², 17 000 m² and 17 000 m²) from two cayes on the atoll were selected to investigate the effect of survey altitude. A linear regression demonstrated that for every 1 m increase in survey altitude, there was a ~1% decrease in the overall classification accuracy. A low survey altitude of 75 m produced a higher classification accuracy for thematic maps and increased the representation of mangrove, seagrass and sand. The variability in classified cover was driven by altitude, although the direction and extent of this relationship was specific to each class. For coral and sea, classified cover decreased with increased altitude. Mangrove classified cover was non-sensitive to altitude changes, demonstrating a lesser need for a consistent survey altitude. Sand and seagrass had a greater sensitivity to altitude, due to classified cover variability between altitudes. Our findings suggest that survey altitude should be minimized when classifying tropical marine environments (coral, seagrass) and, given that most fixed-wing UAVs are restricted to a minimum altitude of 70 m, we recommend an altitude of 75 m. Survey altitude should be a major consideration when targeting habitats with greater sensitivity to altitude variability.

Introduction

Marine coastal habitats offer many important ecosystem services, including food security (Hicks et al. 2019), coastal protection (Spalding et al. 2014) and carbon sequestration (Lee et al. 2014). Coral reefs and seagrass meadows are two of the most productive ecosystems in the coastal zone, and are considered particularly vulnerable to climate change (IPCC 2019; Ramesh et al. 2019). Marine spatial planning

is increasingly undertaken to improve the ecological resilience of ecosystems and their associated services. Fine-scale monitoring, as a component of spatial planning (Collin et al. 2018), is used to assess the status of marine habitats and quantify the changes in spatial extent. Monitoring is necessary in order to identify and mitigate changes in ecosystem health. Habitat mapping is a fundamental component in spatial planning and provides an inventory of habitat types, monitors habitat fragmentation and logs

seascape evolution (Saul and Purkis 2015). Habitat maps provide critical information for management plans and the establishment of conservation areas within marine protected areas (MPAs; Kobryn et al. 2013).

Until recently, satellite-based remote sensing was the primary method of capturing moderate (10–100 m) to high-resolution (1–10 m) aerial imagery (Hedley et al. 2016). Even with significant improvements in spatial resolution over the last decade, satellites cannot provide the sub-metre accuracy required to map moderate-to-fine-scale coastal changes (Ventura et al. 2018). Technological advances have led to the development of lightweight (<10 kg), unmanned aerial vehicles (UAVs) equipped with consumer grade cameras (Anderson and Gaston 2013; Duffy et al. 2018a). UAV uses include environmental monitoring (Koh and Wich 2012), and are used as tools for enforcement, surveillance and behaviour modification in a management context (Mulero-Pázmány et al. 2014; Rees et al. 2018). UAVs have the ability to capture imagery with pixel sizes in the order of centimetres, commonly a spatial resolution of 2–5 cm (Papakonstantinou et al. 2016; Topouzelis et al. 2017; Duffy et al. 2018b; Ventura et al. 2018). High-resolution aerial imagery enables the fine-scale heterogeneity of marine environments to be mapped (Murfitt et al. 2017).

UAV design is of two broad categories: fixed-wing and multi-rotor. Flight endurance is higher for fixed-wings (≥ 45 min). Multi-rotors have a short flight time of ~20–30 min (Tahar 2015; Mesas-Carrascosa et al. 2016; Liu et al. 2018; Ventura et al. 2018), due to their vertical take-off and landing (VTOL) capability. The range of fixed-wings often exceeds that of multi-rotors (Rees et al. 2018). Multi-rotors can travel up to 2 km from launch point (DJI Phantom 3 Professional; Schofield et al. 2017), and have a coverage of 65 ha (DJI Phantom 2 Vision; Marcaccio et al. 2016), in comparison to a coverage of 281 ha for a fixed-wing UAV (sensefly eBee; Marcaccio et al. 2016). As recommended for fixed-wing UAV use, the minimum survey altitude for operation is 70 m. Multi-rotors can survey at a much lower altitude depending upon national regulatory frameworks that impose restrictions (Ventura et al. 2018). UAVs possess low running costs, survey repeatability, a high level of automation and a flexibility with the timing/frequency of image capture (Papakonstantinou et al. 2016; Joyce et al. 2019). Previous studies have demonstrated that fixed-wings are practical platforms for collecting very high-resolution (VHR) imagery (<10 cm pixel⁻¹; Getzin et al. 2012; Long et al. 2016), and producing a high accuracy (>70%) in object-based classification (Rau et al. 2012).

Designating a suitable image-processing workflow is a prerequisite for the successful classification of aerial imagery into a thematic habitat map (Lu and Weng 2007).

Thematic maps are classified orthomosaics, representing the key tropical habitat types of a seascape. With the introduction of VHR aerial imagery, a key shift from pixel-based to object-based image analysis (OBIA) has been made within the habitat mapping community. This allows for the segmentation of fine-scale objects within complex environments (Leon and Woodroffe 2011). In OBIA, the heterogeneity of the pixels making up an object are defined by the 'scale' parameter; a higher scale value corresponds to larger and fewer heterogeneous objects (Ventura et al. 2018). Image objects are also delineated by their geometric properties; the weighting of this factor is controlled by the 'shape' and 'compactness' parameters (Ventura et al. 2018). Extensive testing of algorithms in the literature has highlighted the algorithms of Random Trees (RT) and Support Vector Machine (SVM) for their good performance (Zhang 2015), producing a high classification accuracy (Wahidin et al. 2015; Cabili et al. 2018; Mohamed et al. 2018). RT is a simplified version of random forest, which looks for optimal decision trees to split samples into smaller subdivisions (Zhang et al. 2013). SVM builds a model through analysing data and recognizing patterns, to define the optimal hyperplane to categorize data.

Few habitat mapping studies have investigated OBIA classification accuracy under different altitudes, with those that do reporting conflicting results. Tahar (2015) investigated the accuracy of slope mapping results from a UAV, measured through root mean square error (RMSE). An increase in altitude increased the accuracy of the slope. The average RMSE decreased from ~0.91 m (40 m) to ~0.46 m (80 m). In Udin and Ahmad (2014), an increase in altitude decreased the accuracy of large-scale stream mapping. An average RMSE of ~0.25 m (40 m) increased to ~0.30 m (100 m). These two studies map contrasting environments and may indicate that lower survey altitudes are required for mapping freshwater/marine environments, as opposed to terrestrial environments, in order to contend with factors affecting image quality; for instance, optical refractive distortion of the water surface, and strong water movements in shallow depths may mask submerged features. A lower altitude equates to a higher resolution which allows more detailed information to be gathered, this can still be hindered by an uneven water surface. The above studies are the only ones, to our knowledge, that report habitat classification accuracy with UAV altitude.

Habitat boundaries have been shown to be a source of variability in classification due to algorithmic difficulties with discerning between adjacent habitat types (Saul and Purkis 2015). It follows that distinguishing contrasting habitats and classifying them through OBIA is partly dependent upon image resolution, and therefore altitude.

Ventura et al. (2018) achieved a high overall classification accuracy of 85%, and a kappa index of agreement of 83%, from a comparatively low altitude of 40 m (and a resolution of ~ 3 cm pixel⁻¹). This good match between classification and the original aerial imagery enabled the identification of spectrally different features within a complex area of seagrass. Although high resolutions are therefore currently recommended, as a rule, it remains unclear whether classification accuracy changes with altitude, or whether classified habitat varies in sensitivity to altitude.

The potential trade-off between the classification accuracy of thematic maps from a tropical marine seascape and altitude has yet to be the focus of a formal evaluation. Evaluating the effect of altitude on classification accuracy and habitat classification would help inform UAV-based, habitat survey design. Without this evaluation it remains unclear how much accuracy may be gained by increasing or decreasing survey altitude.

The aim of this study was to investigate the ecological application of fixed-wing UAVs for tropical marine habitat classification, at different survey altitudes. We conducted our trials at two sites on the Turneffe Atoll, Belize, aiming to address the following objectives:

- 1 Obtain high-resolution aerial imagery from fixed-wing UAV surveys. Create orthomosaics and thematic habitat maps displaying tropical marine habitats, using the RT or SVM algorithm.
- 2 Use in-situ georeferenced images from snorkel-based surveys as ground validation to train OBIA classification and assess classification accuracy.
- 3 Determine the effect of survey altitude on the classification accuracy of thematic maps (overall accuracy), and the classification accuracy of individual classes (KIA).
- 4 Determine whether there are differences among classes in terms of how sensitive their classification is, and how it varies with altitude changes.

Materials and Methods

Study sites

UAV surveys were conducted on the Turneffe Atoll, Belize. The atoll is an ecological hotspot for marine biodiversity and was established as a Marine Reserve in 2012 (Belize Fisheries Department 2012). The atoll was chosen due to its shallow-reef ecosystems within a connected seascape. The atoll remains unmapped by UAV technology for habitat classification. The seascape present at the study site was of a scale suitable for UAV survey. The seascape featured sparse algae/sand, seagrass beds, coastal fringe mangrove, shallow coral reef, and spur and groove coral reef (Map 8, Belize Fisheries Department 2012). The

two sites surveyed were Cockroach Caye (17.4956°N, 87.7718°W) and Calabash Caye (17.2828°N, 87.8116°W; Fig. 1). Calabash Caye and Cockroach Caye are small sand cayes located on the inner edge of the reef flats, in a water depth of 0.3–0.6 m (Belize Fisheries Department 2012). They experience a micro-tidal tidal exchange of an estimated 30–50 cm (Belize Fisheries Department 2012). Calabash Caye is part of the General Use Zone encompassing the atoll and was the headquarters for this investigation (HQ). Cockroach Caye (CC) is part of the Cockroach-Grassy Caye Special Management Area (Zone II B), extending into the Dog Flea Conservation Zone (Zone II A; Belize Fisheries Department 2012).

UAV system specifications

We deployed a fixed-wing water-landing UAV fitted with a Sony RX0 1.0" survey camera, orientated 10 degrees off-nadir to provide aerial imagery with a larger field of view and to avoid sun glint while the sun is high (Table A1; Wang and Bailey 2001; Joyce et al. 2019; Schiele and Letessier 2019). Each survey mission was pre-programmed using the open-source software *Mission Planner* (ArduPilot Development Team 2019). Aerial imagery was geotagged retrospectively in *Mission Planner*, using the image timestamp and the UAV telemetry log.

Data collection

Six flights were conducted during late afternoon hours between 1400 and 1630 h, mostly at a sun elevation angle of between 30 degrees and 45 degrees, in order to minimize sun glint (Finkbeiner et al. 2001; Mount 2005; Hodgson et al. 2013). This equated to a total survey time of 1 h 28 min 15 s (Table A2). The sea state remained constant during each survey, and ranged between Beaufort sea state 2 and 3 for all flights. Wind speed at the start of flights ranged from 10.8 to 22.3 kph and largely decreased to 0.1–19.8 kph at the end of flights. This equated to an acceptable average wind speed of 11.55 kph (Finkbeiner et al. 2001). The water clarity during flights was largely affected by sun glint. On an uneven water surface this creates blind spots (Doukari et al. 2019). Surface waves hindered subsurface visibility and resulted in the blurring of some aerial imagery. At each site, aerial surveys were conducted at three altitudes above mean sea level (AMSL) to achieve varying ground sample distances (GSDs). A low GSD corresponds to a high-resolution image. An inter-photo distance of 5 m ensured a high front overlap of images (Table 1). Three 50 m tape transects were snorkel surveyed at each site. From this, representative data of the benthic environment proximal to the aerial survey area were obtained to cover as many existing

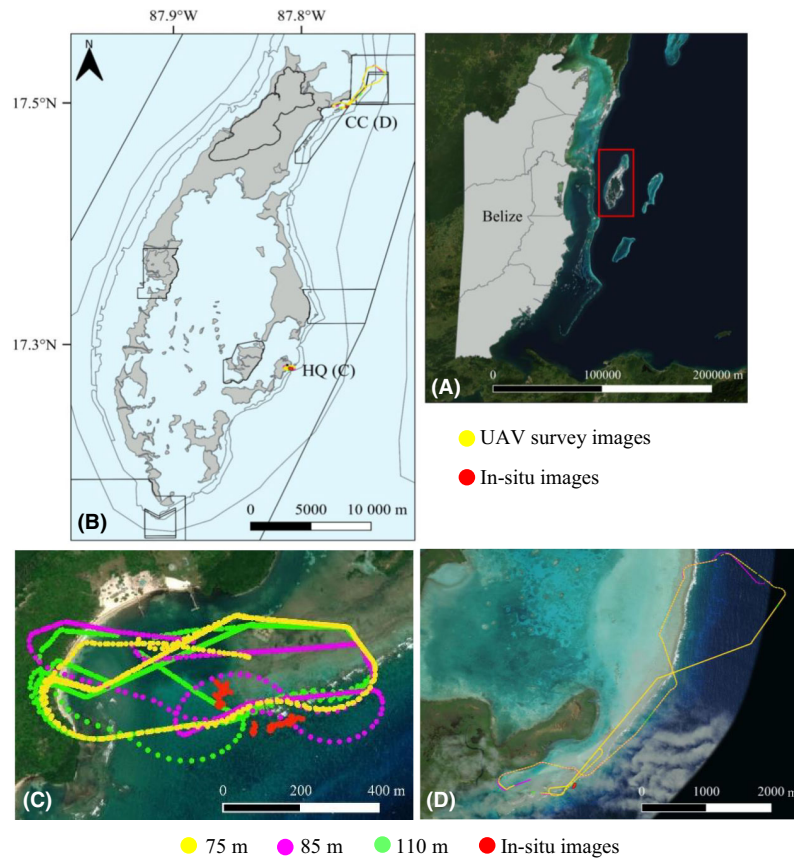


Figure 1. Location of the Turneffe Atoll (A) with its protected areas and UNESCO ecosystems (marked by black lines on B, shapefiles taken from Meerman and Clabaugh (2017)), coordinates of UAV survey images marked in yellow and in-situ images marked in red on B. At Calabash Caye (C) and Cockroach Caye (D), UAV survey images were taken at an altitude of 75 m (marked in yellow), 85 m (pink) and 110 m (green), in-situ images marked in red (QGIS Development Team 2018) .

habitat types as possible. During snorkel surveys, in-situ georeferenced images were taken every second by a Garmin Virb Ultra 30 GoPro, held just below the water surface (Fig. 2).

Orthomosaic generation

The photogrammetric software of *3DF Zephyr Aerial v. 4.353* (3Dflow 2015) generated true orthomosaics from mesh via a reference axis. The batch-processing tool was used to mosaic the aerial imagery for each survey. Orthomosaics were geometrically corrected during camera alignment to remove spatial distortions, resulting in the removal of aerial imagery that was significantly distorted and/or affected by sun glint. This largely prevented sun glint from reducing the quality of the orthomosaics and affecting classification. This explains the difference between the number of images that were captured during the survey, and the number of images that were aligned to form the orthomosaic (Table 1).

Object-based image analysis and accuracy assessment

Semi-automatic OBIA using machine-learning algorithms was performed on the orthomosaics in *eCognition Developer v. 9.5.0* (Trimble 2018). A methodology framework was followed (Figure A1). The following parameters were used in automated *multi-resolution segmentation*: scale: 25, compactness: 0.8 and shape: 0.1. Smaller objects were merged into larger objects through the bottom-up approach using a structured trial-and-error process. The classes of coral, mangrove, sea, sand and seagrass were chosen for the class hierarchy (Table 2; Belize Fisheries Department 2012). Supervised classification of these classes based on the thresholds of image features (mean RGB values, mean brightness and standard deviation RGB), was performed using the SVM or RT machine-learning algorithm. The algorithm was selected by its visual classification result and its relative classification accuracy defined by overall accuracy (OA) and kappa

Table 1. The area and resolution of orthomosaics generated on *Zephyr* for Calabash Caye (HQ) and Cockroach Caye (CC), Turneffe Atoll at the survey altitudes of 75 m, 85 m and 110 m. Aerial surveys conducted between 21/02/19 and 01/03/19. GSD (resolution) based on area of the orthomosaic

Orthomosaic	No. images (aligned/ captured)	Area (width x height, pixels)	GSD (cm pixel ⁻¹)	Overlap (%)
HQ 75 m	303/1022	2785 × 5318	4.62	93.10
HQ 85 m	387/752	4499 × 2924	3.24	93.91
HQ 110 m	2089/3595	4950 × 4027	3.18	95.29
CC 75 m	423/3062	3485 × 10 424	3.69	93.10
CC 85 m	750/2243	24 901 × 8026	0.59	93.91
CC 110 m	486/2050	11 007 × 7993	1.71	95.29

index of agreement (KIA). Manual classification through selecting individual objects is often carried out to achieve a meaningful accuracy yet is considered time consuming and labour intensive, so full or partial automation is advisable (Zhang et al. 2013; Saul and Purkis 2015). In this study a combination of semi-automatic OBIA and manual classification was used. Non-mosaiced objects or objects recognized as infrastructure (pier and base at HQ, Figure A4) in the orthomosaics were manually selected, and classified as N/A to avoid being wrongly classified as habitat in semi-automatic OBIA.

The photo-interpretation method was used to assign samples collected from the field (in-situ georeferenced images) and from the orthomosaics on QGIS to the classes of the hierarchy. This ensured that any classes of the hierarchy that were not represented by samples from the field, were covered with samples selected on QGIS. Samples were split equally into an independent validation and a training sample set, as opposed to using all reference points to support both interpretation and mapping (Lathrop et al. 2013; Figure A2). Training samples trained object-based classification. Validation samples acted as reference data in error matrices to compare classified objects with sample objects, to calculate the classification accuracy (OA and KIA) of thematic maps. As defined by Ventura et al. (2018), OA is the proportion of correctly classified objects of the total sample size. The result of performing KIA is a KHAT statistic (κ an estimate of kappa), which is a measure of the agreement between the classification results and the reference data, taking into consideration omission and commission errors (Ventura et al. 2018). The assessment of classification performance measured by the KHAT statistic followed the proposed categories of Congalton and Green (2002), and Sim and Wright (2005): poor (≤ 0), slight (0.01–0.20), fair (0.21–0.40), moderate (0.41–0.60), substantial (0.61–0.80) and almost perfect (≥ 0.81).

Statistical analysis

Two subsets at HQ and one subset at CC were selected to represent the habitats present at the two study sites. A linear regression model was fitted to determine whether a linear relationship exists between altitude and overall classification accuracy. The classes of coral and sea were not included in the linear statistics as the subset area chosen (Fig. 4) was only covered by the transects flown at the survey altitudes of 85 and 110 m. All analyses were conducted in *RStudio* (R Core Team 2018).

Results

Orthomosaics and thematic habitat maps of Calabash Caye and Cockroach Caye

The orthomosaics revealed a high level of detail, including the dominant habitat types characteristic of the coastal seascape studied in this investigation (Figure A3). The dominant habitats are displayed in the in-situ georeferenced images (Fig. 2), which are examples of ground validation samples used in the OBIA process. The algorithm chosen to classify the aerial imagery at each site was dependent upon its relative classification accuracy. The RT algorithm was selected to classify the subsets of HQ (Fig. 3, 4). The SVM algorithm was selected to classify the subsets of CC (Fig. 5).

Altitude effects at Calabash Caye and Cockroach Caye

A Shapiro–Wilk normality test demonstrated that the classification accuracy data of this investigation did not significantly deviate from a normal distribution ($P > 0.05$). GSD decreased with a decrease in altitude, corresponding to a higher resolution at a lower survey altitude (Table 1). For every 1 m increase in altitude, there was a ~1% decrease in the OA of classification (Fig. 6). The KIA also decreased with an increase in altitude. Classification performance was termed almost perfect at 75 m and had a high agreement to the reference data with a KHAT statistic of ~0.81. Performance then decreased to moderate at 85 m (0.60) and fair at 110 m (~0.21). The negative linear relationship between altitude and OA was significant ($r^2 = 0.954$, $df = 4$, $P < 0.05$). The coefficient estimate did not vary greatly from the actual value with a standard error of ~0.095. The model explained a high amount of the observed variance in overall accuracy.

Overall, the best classification performance was at a lower survey altitude of 75 m, or 85 m for coral and sea. With an increase in altitude, a less favourable classification performance was evident (Table 3). Classified habitat varied by both altitude and class. Certain habitats were favoured

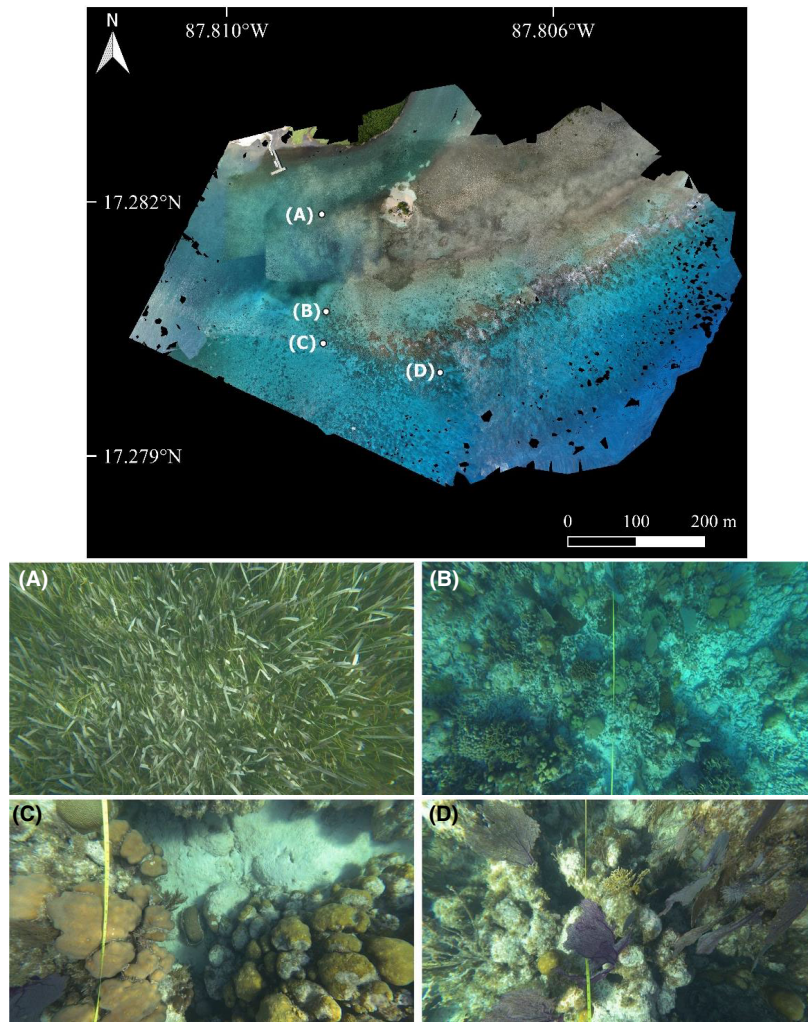


Figure 2. High-resolution orthomosaic of Calabash Caye at 110 m ($3.18 \text{ cm pixel}^{-1}$), with some of the dominant marine habitats recorded during snorkel-surveys: dense seagrass from the genera *Thalassia* and *Syringodium* (A), coral expanse featuring dead corals (reef crest, B), sand amongst coral patch featuring hard corals (reef crest, C) and soft coral and algae (foreereef, D).

Table 2. Class, description and legend key for thematic habitat maps (Fig. 3, 4, 5 and Figure A5)

Key	Class	Description
■	Coral	Areas of seascape covered in coral habitat, mainly surrounding reef crest.
■	Mangrove	Coastal area dominated by mangroves. Predominant species on the atoll is <i>Rhizophora mangle</i> .
■	Sea	Areas where other habitat is unidentifiable, including the shallow waters of the back reef and the deeper water of the fore reef.
■	Sand	Including exposed and submerged sand, mainly within the back reef environment.
■	Seagrass	Dense expanses of seagrass comprised primarily of the genus <i>Thalassia</i> and <i>Syringodium</i> .
■	N/A	Areas of the seascape with no aerial imagery, including infrastructure at HQ.

(coral and sand), disfavoured (seagrass and sea) or indifferent (mangrove) with an increase in altitude (Figure A5). Seagrass was best represented at a lower altitude, with a high

classified cover at 75 m. Whereas, sand was best represented at a higher altitude of 110 m. Mangrove maintained a relatively consistent classified cover across altitude and

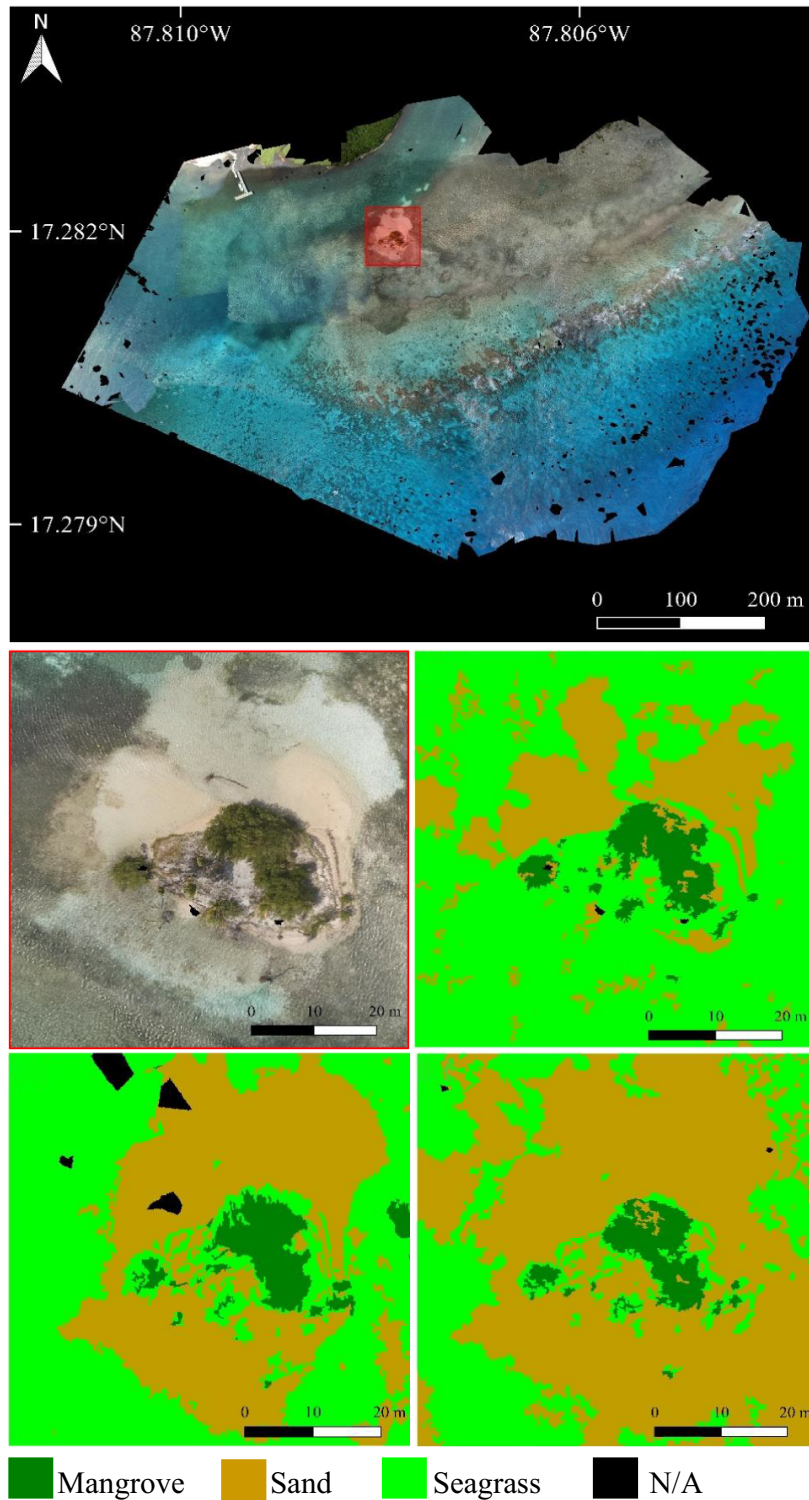


Figure 3. Specified subset (A) from orthomosaic (110 m) at Calabash Caye, classified by the RT algorithm in OBIA at the survey altitudes of 75 m (B), 85 m (C) and 110 m (D). Thematic subsets detail the four cover classes of mangrove, sand, seagrass and N/A. Subset area: 621 × 646 pix, 4000 m².

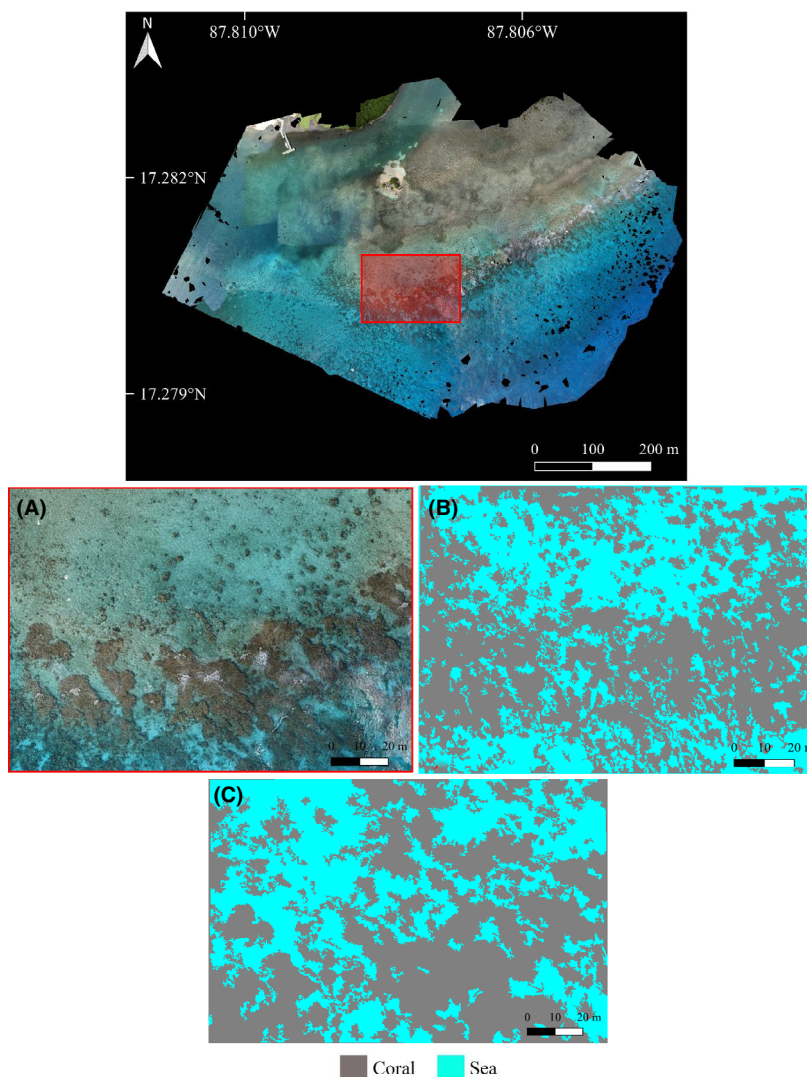


Figure 4. Specified subset (A) from orthomosaic (110 m) at Calabash Caye, classified by the RT algorithm in OBIA at the survey altitudes of 85 m (B) and 110 m (C). Thematic subsets detail the two cover classes of coral and sea. Subset area: 1152 × 860 pix, 17 000 m².

appeared non-sensitive to altitude changes. Habitat classified as coral and sea did not vary greatly between the altitudes of 85 m and 110 m. Changes in classified cover were driven by altitude and varied by class. Sand and seagrass had the largest variability in habitat classified, showing large differences in classification between survey altitudes. Coral and sea have a reduced variability in classified cover, with the lowest variability for mangrove (Fig. 7).

Discussion and Conclusions

Main findings and recommendations

Our study quantifies the implications of survey altitude on habitat classification accuracy, thus making our results

applicable to other UAV-based studies conducting tropical marine habitat classification. Results are especially relevant to those using fixed-wing UAVs, as we present our ideal survey altitude to be only 5 m above the minimum survey altitude of 70 m recommended for fixed-wing UAV use. We demonstrate that the classification accuracy of thematic maps scales negatively with altitude. A lower altitude gave the highest overall accuracy for thematic maps, and best represented the most habitats in a seascape through a high classification performance, measured by KIA. An important consideration is that classification performance (KIA) can increase/decrease with an increase in altitude or remain relatively stable, depending on the habitat. We also found that certain habitats showed variability in their classified cover and a level of sensitivity to altitude changes.

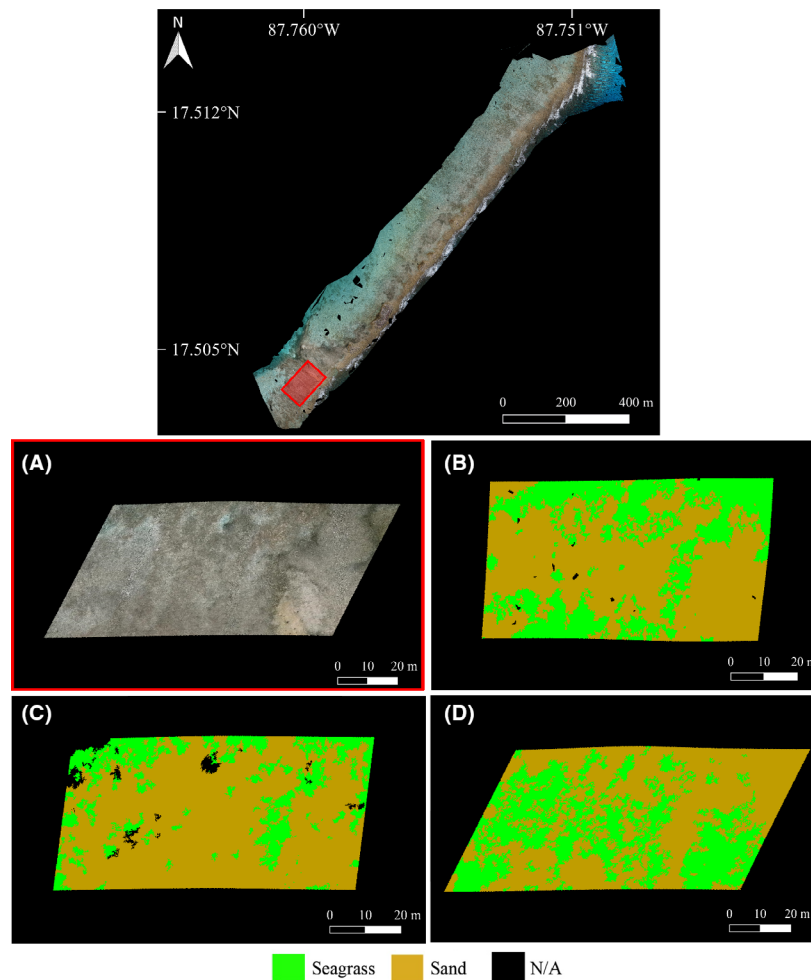


Figure 5. Specified subset (A) from orthomosaic (110 m) at Cockroach Caye, classified by the SVM algorithm in OBIA at the survey altitudes of 75 m (B), 85 m (C) and 110 m (D). Thematic subsets detail the three cover classes of seagrass, sand and N/A. Subset area: 551 × 924 pix, 17 000 m².

Orthomosaics and thematic maps of Calabash Caye and Cockroach Caye

Characteristic of the tropical seascape displayed in the high-resolution orthomosaics of HQ, is the reef crest of low relief spur and groove (Map 8, Belize Fisheries Department 2012). From the reef crest, patch reef extends merging into seagrass and submerged sand substratum adjacent to the crest on the back reef, or a rubble seabed sloping into deeper water on the fore reef. Thematic maps confirmed the transition of habitats in the HQ seascape (Figure A5). The habitats of seagrass, submerged sand substratum on the back reef, coral on the reef crest and coastal mangrove were especially visible at 75 m and 110 m. The coral-dominated zones at HQ are defined by the dominance of different coral species (Blanco and Ricketts 2017). *Siderastrea siderea*, *Porites asteroides* and

Undaria agaricitis are reported to be the most abundant coral species on the atoll, with their highest cover on the back reef (Blanco and Ricketts 2017). Coral species or morphologies were not distinguishable from the thematic maps. Small features within a seascape, such as coral, require low-altitude surveillance, high image overlap and low GSD (Joyce et al. 2019). This study demonstrated the trade-off between desired resolutions and a survey altitude which is both optimal for classification accuracy, safe for operating, and covers a seascape scale. The highest orthomosaic resolution was at a survey altitude of 75 m, which also produced the best overall accuracy for classification. Future considerations would be a crosshatch flight plan to allow for high side and front overlap of images. This would decrease edge effects on orthomosaics and increase classification accuracy, as often there is a decrease in accuracy along edges due to limited overlap. The

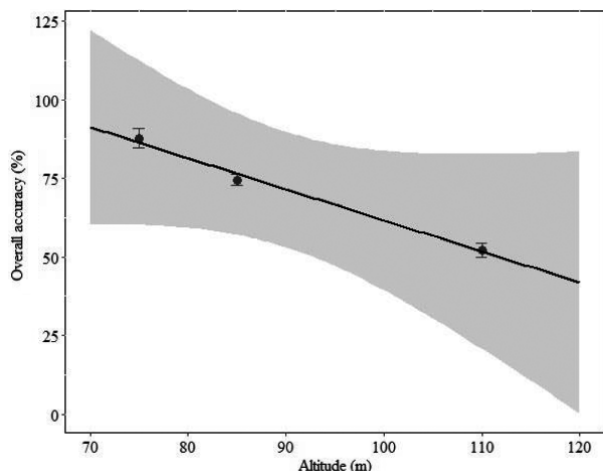


Figure 6. Average overall accuracy (%; \pm SE) of classifications made at the survey altitudes of 75 m, 85 m and 110 m, with 95% confidence interval. Data refers to classified subset areas from Calabash Caye and Cockroach Caye (Fig. 3, 5). Class N/A not included.

Table 3. Assessment of classification performance determined by kappa index of agreement (KIA; KHAT statistic in brackets), of classes classified at the survey altitudes of 75 m, 85 m and 110 m

Class	Altitude (m)		
	75	85	110
Mangrove	Almost perfect (1)	Moderate (0.45)	Moderate (0.45)
Sand	Moderate (~0.56)	Substantial (~0.73)	Moderate (0.5)
Seagrass	Almost perfect (1)	Moderate (~0.52)	Poor (~ -0.35)
Coral	-	Almost perfect (1)	Fair (~-0.33)
Sea	-	Substantial (~0.66)	Moderate (0.5)

centre of orthomosaics have a higher positional accuracy due to more overlapping images (Hung et al. 2019).

Altitude effects at Calabash Caye and Cockroach Caye

The algorithm and survey altitude that produced the highest overall accuracy for thematic maps, and achieved the best classification performance for the most classes, are considered most suitable. The RT algorithm was chosen to classify more subsets due to a higher classification accuracy. A survey altitude of 75 m was optimal as it best represented the most classes and produced the highest overall classification accuracy. Similarly, a lower altitude of 70 m with 90% image overlap surveyed by a fixed-wing UAV in Jeong et al. (2018), produced the highest accuracy (RMSE). In Perroy et al. (2017), a lower survey altitude of 30 m above ground level produced the finest

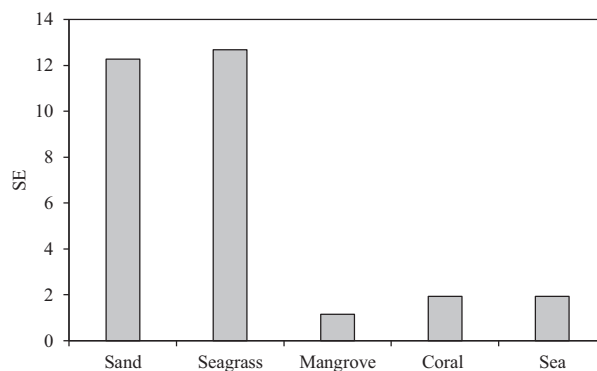


Figure 7. Standard error of total class classified (%) at the survey altitudes of 75 m, 85 m and 110 m for the classes of sand, seagrass, mangrove, coral, and sea. Data refers to classified subset areas from Calabash Caye and Cockroach Caye (Fig. 3, 4 and 5). Class N/A not included.

resolution imagery in a terrestrial survey and a 100% detection rate of invasive flora. Detection rates progressively declined with an increase in altitude due to coarser-resolution aerial imagery. In accordance with this study, a lower survey altitude is linked to higher-resolution imagery which in turn corresponds to a more accurate classification. However, high-resolution imagery from a lower altitude is not consistent with more objects classified for all classes of the hierarchy. This may be explained by the low spectral separation between objects of certain classes (Ventura et al. 2018). In our investigation, a low spectral separation between adjacent objects led to low capacity to discern between exposed and submerged sand, and between coral and rubble. At our study sites, mangrove was the dominant coastal terrestrial vegetation to be classified, and was spectrally different from surrounding habitat covers. Mangrove was mainly confined to the coastline in aerial imagery taken from the study sites or appeared as an outcrop surrounded by sand (Fig. 3). There was no requirement for demarcation between vegetation community boundaries, which can be a source of inaccuracy in classification due to high spectral and spatial variability (Heenkenda et al. 2014). The collection of reliable information for the classification of terrestrial and coastal environments is challenged by weather and sea state conditions, with the main environmental limiting factor in this investigation being sun glint. The distortion of aerial imagery of marine habitats can be seen in the orthomosaics. Procedures for collecting accurate marine information in the optimal survey conditions need to be set in place (Doukari et al. 2019). The consistently high classification performance and the reduced variability in classified cover of mangrove, demonstrated this habitat to be non-sensitive to altitude effects. This is relevant for

habitat mapping purposes as conclusions based on classified mangrove can be made confidently across survey altitude, and there is a lesser need for a consistent altitude during flight. The variability in objects classified as sand, seagrass, coral and sea demonstrated these classes to be sensitive to altitude changes. The classification of sand and seagrass was particularly prone to altitude changes, due to a large variability in classified cover between survey altitudes. The sensitivity of sand and seagrass to altitude changes may prove challenging in making conclusions based on their cover and expanse. An inconsistent survey altitude could lead to variability in classification, and the over-representation or under-representation of certain habitats. The manual selection of samples in this investigation created a better classification view, a higher OA and permitted sand and seagrass to be delineated. Additional samples may facilitate accurate classification at an unfavourable survey altitude, or in areas where environmental factors distort imagery, which is an issue presented at all altitudes. Procedures for determining the optimum sample number for effective OBIA classification should be implemented in future UAV studies.

Conclusions

Fixed-wing UAVs can be applied for tropical marine habitat classification in remote sensing. They can produce VHR aerial imagery for developing habitat maps for marine spatial planning purposes. This is relevant to MPAs, including the Turneffe Atoll, which will be designating more preservation zones to increase the percentage of protected waters in Belize from 4.5% to 11.6% (BBN 2019). We evaluated the effects of altitude on classification accuracy and habitat classification. A linear relationship between altitude and overall accuracy confirmed a lower altitude to produce a better classification result. A lower altitude of 75 m best represented the tropical marine habitats of the seascape, through a high classification performance. These findings suggest that altitude should be minimized for classifying marine environments. This excludes mangrove where classified cover was not sensitive to altitude changes, shown by a consistent KIA at 85 and 110 m. Changes in classified cover variability could be driven by altitude and are shown to be specific to class. Studies should consider which classes are sensitive to changes in classified cover between different altitudes, such as sand and seagrass. Given that most fixed-wing UAVs are restricted to a minimum altitude of 70 m, we recommend an altitude of 75 m for tropical environments. Technically, to better understand the implications of the results, future work should feature a consistent crosshatch flight plan, a guideline OBIA procedure for repeatable feature selection (Ventura et al. 2018), and the

collection of GCPs. This would enable the investigation to be extended to more sites on the atoll and enable the production of habitat maps to monitor fragmentation and log seascape evolution (Saul and Purkis 2015).

Acknowledgments

We thank Dr. Louis Cliff and Jessica Wright from the School of Computer Science and Electronic Engineering (CSEE), for their assistance with mosaicing the aerial imagery into orthomosaics. This research was funded by the Bertarelli Foundation and the Marine Management Organisation (MMO), and we are grateful for their support. We thank the Turneffe Atoll Sustainability Association (TASA) for hosting SE, MS and TBL in the field, and for the warm welcome. We thank Mauricio Ortiz, Julian Villada and the rest of the Aeromao team for their excellent technical assistance. We thank 3WiseMonkeys and Sarah Keynes (MMO) for field support and friendship.

Conflict of Interest

All authors have no conflict of interest to declare.

References

- Anderson, K., and K. J. Gaston. 2013. Lightweight unmanned aerial vehicles will revolutionize spatial ecology. *Front. Ecol. Environ.* **11**, 138–146.
- ArduPilot Development Team. 2019. Mission Planner (Version 1.3.62) [Computer program]. Available at: <http://ardupilot.org/planner/docs/mission-planner-installation.html> (Accessed: 19 February 2019).
- BBN. 2019. Cabinet approves expansion of Fisheries Replenishment (No-Take) Zones. Available at: <https://www.breakingbelizenews.com/2019/04/03/cabinet-approves-expansion-of-fisheries-replenishment-no-take-zones/> (Accessed: 5 April 2019).
- Belize Fisheries Department. 2012. *Turneffe atoll marine reserve management plan*. Wildtracks, Belize City. Available at: <http://fisheries.gov.bz> (Accessed: 6 February 2019).
- Blanco, I., and L. C. Ricketts. 2017. Turneffe atoll marine reserve ecosystem health monitoring 2014. Available at: http://eprints.uberibz.org/1626/1/Turneffe_Ecosystem_Health_Report_2014_summary.pdf (Accessed: 25 July 2019).
- Cabili, J. R. C., M. A. J. Torres, M. T. T. Ignacio, K. M. F. Dagoc, and J. Q. Guihawan. 2018. Object-based image analysis for extraction of mangrove forests in rehabilitated areas of Bacolod, Lanao Del Norte, Philippines using lidar data and GIS. *Res. J. Appl. Sci.* **14**, 6–10.
- Collin, A., C. Ramambason, Y. Pastol, E. Casella, A. Rovere, L. Thiault, et al. 2018. Very high resolution mapping of coral reef state using airborne bathymetric LiDAR surface-intensity and drone imagery. *Int. J. Remote Sens.* **39**, 5676–5688.

- Congalton, R. G., and K. Green. 2002. *Assessing the accuracy of remotely sensed data: principles and practices*. CRC Press, Boca Raton.
- 3Dflow. 2015. 3DF Zephyr Aerial (Version 4.353) [Computer program]. Available at: <https://www.3dflow.net/3df-zephyr-feature-comparison/>. 3Dflow SRL, Strada le Grazie 15, 37134 Verona, Italy.
- Doukari, M., M. Batsaris, A. Papakonstantinou, and K. Topouzelis. 2019. A protocol for aerial survey in coastal areas using UAS. *Remote Sens.* **11**, 1–19.
- Duffy, J. P., A. M. Cunliffe, L. DeBell, C. Sandbrook, S. A. Wich, J. D. Shutler, et al. 2018a. Location, location, location: considerations when using lightweight drones in challenging environments. *RSEC* **4**, 7–19.
- Duffy, J.P., L. Pratt, K. Anderson, P. E. Land, and J. D. Shutler. 2018b. Spatial assessment of intertidal seagrass meadows using optical imaging systems and a lightweight drone. *Estuar. Coast. Shelf Sci.* **200**, 169–180.
- Finkbeiner, M., B. Stevenson, and R. Seaman. 2001. Guidance for benthic habitat mapping: an aerial photographic approach. Charleston: U.S. NOAA Coastal Services Center. Available at: U.S. National Oceanic and Atmospheric Administration (Accessed: 22 February 2020).
- Getzin, S., K. Wiegand, and I. Schöning. 2012. Assessing biodiversity in forests using very high-resolution images and unmanned aerial vehicles. *Methods Ecol. Evol.* **3**, 397–404.
- Hedley, J., C. Roelfsema, I. Chollett, A. Harborne, S. Heron, S. Weeks, et al. 2016. Remote sensing of coral reefs for monitoring and management: a review. *Remote Sens.-basel* **8**, 118.
- Heenkenda, M., K. Joyce, S. Maier, and R. Bartolo. 2014. Mangrove species identification: comparing worldview-2 with aerial photographs. *Remote Sens.* **6**, 6064–6088.
- Hicks, C. C., P. J. Cohen, N. A. J. Graham, K. L. Nash, E. H. Allison, C. D’Lima, et al. 2019. Harnessing global fisheries to tackle micronutrient deficiencies. *Nature* **540**, 30–34.
- Hodgson, A., N. Kelly, and D. Peel. 2013. Unmanned aerial vehicles (UAVs) for surveying marine fauna: a dugong case study. *PLoS ONE* **8**, 1–15.
- Hung, I., D. Unger, D. Kulhavy, and Y. Zhang. 2019. Positional precision analysis of orthomosaics derived from drone captured aerial imagery. *Drones* **3**, 46.
- IPCC. 2019. Summary for policymakers. In: *IPCC special report on the ocean and cryosphere in a changing climate* [H.-O. Pörtner, D.C. Roberts, V. Masson-Delmotte, P. Zhai, M. Tignor, E. Poloczanska, K. Mintenbeck, M. Nicolai, A. Okem, J. Petzold, B. Rama, N. Weyer (eds.)]. In press.
- Jeong, E., J. Y. Park, and C. S. Hwang. 2018. Assessment of UAV photogrammetric mapping accuracy in the beach environment. *J. Coastal Res.* **85**, 176–180.
- Joyce, K. E., S. Duce, S. M. Leahy, J. Leon, and S. W. Maier. 2019. Principles and practice of acquiring drone-based image data in marine environments. *Mar. Freshw. Res.* **70**, 952–963.
- Kobryn, H. T., K. Wouters, L. E. Beckley, and T. Heege. 2013. Ningaloo reef: shallow marine habitats mapped using a hyperspectral sensor. *PLoS ONE* **8**, 1–22.
- Koh, L. P., and S. A. Wich. 2012. Dawn of drone ecology: low-cost autonomous aerial vehicles for conservation. *Trop. Conserv. Sci.* **5**, 121–132.
- Lathrop, R. G., P. Montesano, and S. Haag. 2013. A multi-scale segmentation approach to mapping seagrass habitats using airborne digital camera imagery. *Photogramm. Eng. Remote Sensing* **72**, 665–675.
- Lee, S. Y., J. H. Primavera, F. D. Guebas, K. McKee, J. O. Bosire, S. Cannicci, et al. 2014. Ecological role and services of tropical mangrove ecosystems: a reassessment. *Global Ecol. Biogeogr.* **23**, 726–743.
- Leon, J., and C. D. Woodroffe. 2011. Improving the synoptic mapping of coral reef geomorphology using object-based image analysis. *Int. J. Geogr. Inf. Sci.* **25**, 949–969.
- Liu, Y., X. Zheng, G. Ai, Y. Zhang, and Y. Zuo. 2018. Generating a high-precision true digital orthophoto map based on UAV images. *Isprs. Int. Geo-inf.* **7**, 333.
- Long, N., B. Millescamp, F. Pouget, A. Dumon, N. Lachaussée, and X. Bertin. 2016. Accuracy assessment of coastal topography derived from UAV images. *ISPRS J. Photogramm.* **41**, 1127–1134.
- Lu, D., and Q. Weng. 2007. A survey of image classification methods and techniques for improving classification performance. *Int. J. Remote Sens.* **28**, 823–870.
- Marcaccio, J. V., C. E. Markle, and P. Chow-Fraser. 2016. Use of fixed-wing and multi-rotor unmanned aerial vehicles to map dynamic changes in a freshwater marsh. *J. Unmanned Veh. Syst.* **4**, 193–202.
- Meerman, J., and J. Clabaugh. 2017. Biodiversity and environmental resource data system of Belize. Available at: <http://www.biodiversity.bz> (Accessed: 5 June 2019).
- Mesas-Carrascosa, F. J., M. D. N. Garcia, J. E. Meroño de Larriva, and A. García-Ferrer. 2016. An analysis of the influence of flight parameters in the generation of unmanned aerial vehicle (UAV) orthomosaics to survey archaeological areas. *Sensors* **16**, 1–14.
- Mohamed, H., K. Nadaoka, and T. Nakamura. 2018. Assessment of machine learning algorithms for automatic benthic cover monitoring and mapping using towed underwater video camera and high-resolution satellite images. *Remote Sens.-basel.* **10**, 773.
- Mount, R. 2005. Acquisition of through-water aerial survey images: surface effects and the prediction of sun glitter and subsurface illumination. *Photogramm. Eng. Remote Sens.* **71**, 1407–1415.
- Mulero-Pázmány, M., R. Stolper, L. D. van Essen, J. J. Negro, and T. Sassen. 2014. Remotely piloted aircraft systems as a rhinoceros anti-poaching tool in Africa. *PLoS ONE* **9**, 1–10.
- Murfitt, S. L., B. M. Allan, A. Bellgrove, A. Rattray, M. A. Young, and D. Ierodiaconou. 2017. Applications of

- unmanned aerial vehicles in intertidal reef monitoring. *Sci. Rep-UK* **7**, 1–11.
- Papakonstantinou, A., K. Topouzelis, and G. Pavlogeorgatos. 2016. Coastline zones identification and 3D coastal mapping using UAV spatial data. *ISPRS Int. Geo-inf.* **5**, 75.
- Perroy, R. L., T. Sullivan, and N. Stephenson. 2017. Assessing the impacts of canopy openness and flight parameters on detecting a sub-canopy tropical invasive plant using a small unmanned aerial system. *ISPRS J. Photogramm.* **125**, 174–183.
- QGIS Development Team. 2018. QGIS Geographic Information System (Version 3.4.4-Madeira) [Computer program]. Available at: <http://qgis.osgeo.org> (Downloaded: 22 February 2019).
- R Core Team. 2018. R: A language and environment for statistical computing (Version RStudio 1.0.153) [Computer program]. Available at: <https://www.R-project.org/> (Downloaded: 3 September 2017).
- Ramesh, R., K. Banerjee, A. Paneerselvam, R. Raghuraman, R. Purvaja, and A. Lakshmi. 2019. Importance of seagrass management for effective mitigation of climate change. Pp. 283–299 in R. R. Krishnamurthy, M. P. Jonathan, S. Srinivasalu and B. Glaeser, eds. *Coastal management: global challenges and innovations*. Academic Press, United Kingdom.
- Rau, J. Y., J. P. Jhan, C. F. Lo, and Y. S. Lin. 2012. Landslide mapping using imagery acquired by a fixed-wing UAV. *ISPRS J. Photogramm.* **38**, 195–200.
- Rees, A. F., L. Avens, K. Ballorain, E. Bevan, A. C. Broderick, R. R. Carthy, et al. 2018. The potential of unmanned aerial systems for sea turtle research and conservation: a review and future directions. *Endanger. Species. Res.* **35**, 81–100.
- Saul, S., and S. Purkis. 2015. Semi-automated object-based classification of coral reef habitat using discrete choice models. *Remote Sens-basel.* **7**, 15894–15916.
- Schiele, M. A., and T. B. Letessier. 2019. Amphibious Drone Field Report, Belize. In partnership with the Turneffe Atoll Sustainability Association, the Marine Management Organisation and the Bertarelli Foundation. Available at: <https://www.researchgate.net/publication/334896572> (Accessed: 1 June 2019).
- Schofield, G., K. A. Katselidis, M. K. Lilley, R. D. Reina, and G. C. Hays. 2017. Detecting elusive aspects of wildlife ecology using drones: new insights on the mating dynamics and operational sex ratios of sea turtles. *Funct. Ecol.* **31**, 2310–2319.
- Sim, J., and C. C. Wright. 2005. The kappa statistic in reliability studies: use, interpretation, and sample size requirements. *Phys. Ther.* **85**, 257–268.
- Spalding, M. D., S. Ruffo, C. Lacambra, I. Meliane, L. Z. Hale, C. C. Shepard, et al. 2014. The role of ecosystems in coastal protection: adapting to climate change and coastal hazards. *Ocean Coast Manage.* **90**, 50–57.
- Tahar, K. N. 2015. Multi rotor UAV at different altitudes for slope mapping studies. *ISPRS J. Photogramm.* **40**, 9–16.
- Topouzelis, K., A. Papakonstantinou, M. Doukari, P. Stamatis, D. Makri, and S. Katsanevakis. 2017. Coastal habitat mapping in the Aegean Sea using high resolution orthophoto maps. In *Proceedings of the Fifth International Conference on Remote Sensing and Geoinformation of the Environment (RSCy2017)*, Paphos, Cyprus, 20 – 23 March, 52.
- Trimble. 2018. eCognition Developer (Version 9.5.0) [Computer program]. Available at: <http://www.ecognition.com/suite/ecognition-developer> (Downloaded: 20 July 2019).
- Udin, W. S., and A. Ahmad. 2014. Assessment of photogrammetric mapping accuracy based on variation flying altitude using unmanned aerial vehicle.
- Ventura, D., A. Bonifazi, M. Gravina, A. Belluscio, and G. Ardizzone. 2018. Mapping and classification of ecologically sensitive marine habitats using unmanned aerial vehicle (UAV) imagery and object-based image analysis (OBIA). *Remote Sens-basel.* **10**, 1–23.
- Wahidin, N., V. P. Siregar, B. Nababan, I. Jaya, and S. Wouthuyzen. 2015. Object-based image analysis for coral reef benthic habitat mapping with several classification algorithms. *Procedia Environ. Sci.* **24**, 222–227.
- Wang, M., and S. W. Bailey. 2001. Correction of sun glint contamination on the SeaWiFS ocean and atmosphere products. *Appl. Opt.* **9**, 65–69.
- Zhang, C. 2015. Applying data fusion techniques for benthic habitat mapping and monitoring in a coral reef ecosystem. *ISPRS J. Photogramm.* **104**, 213–223.
- Zhang, C., D. Selch, Z. Xie, C. Roberts, H. Cooper, and G. Chen. 2013. Object-based benthic habitat mapping in the Florida Keys from hyperspectral imagery. *Estuar. Coast Shelf Sci.* **134**, 88–97.

Supporting Information

Additional supporting information may be found online in the Supporting Information section at the end of the article.

Table S1. Error matrix based on validation samples for site HQ, subset area, at survey altitude 75 m. Classification results of RT and SVM algorithm.

Table S2. Error matrix based on validation samples for site HQ, subset area, at survey altitude 85 m. Classification results of RT and SVM algorithm.

Table S3. Error matrix based on validation samples for site HQ, subset area, at survey altitude 110 m. Classification of RT and SVM algorithm.

Table S4. Error matrix based on validation samples for site HQ, subset area no. 2, at survey altitude 85 m. Classification results of RT and SVM algorithm. Mangrove, seagrass and sand were not classified.

Table S5. Error matrix based on validation samples for site HQ, subset area no. 2, at survey altitude 110 m.

Classification results of RT and SVM algorithm. Mangrove, seagrass and sand were not classified.

Table S6. Error matrix based on validation samples for site CC, subset area, at survey altitude 75 m. Classification results of SVM and RT algorithm. Mangrove was not classified.

Table S7. Error matrix based on validation samples for site CC, subset area, at survey altitude 85 m. Classification results of SVM and RT algorithm. Mangrove was not classified.

Table S8. Error matrix based on validation samples for site CC, subset area, at survey altitude 110 m. Classification results of SVM and RT algorithm. Mangrove was not classified.

Table A1. UAV (Aeromao, no date) and survey camera specifications (Sony, 2019).

Table A2. Aerial survey flights conducted between 21/02/19 – 01/03/19 at Cockroach Caye (CC) and Calabash Caye (HQ).

Figure A1. The designated methodology workflow for object-based image analysis in *eCognition*, applied to imagery collected by aerial survey over Calabash Caye and

Cockroach Caye at the survey altitudes of 75 m, 85 m and 110 m.

Figure A2. All photo-interpreted samples, split into validation and training sets, used for the mapping and interpretation of orthomosaics in OBIA at Calabash Caye (A) and Cockroach Caye (B).

Figure A3. True orthomosaics generated on *3DF Zephyr Aerial* from aerial imagery produced at Calabash Caye at a survey altitude of 75 m (A), 85 m (B) and 110 m (C), and Cockroach Caye at a survey altitude of 75 m (D), 85 m (E) and 110 m (F).

Figure A4. Thematic maps displaying classification results of orthomosaics, detailing six cover classes. Orthomosaics of Calabash Caye were classified in OBIA by the SVM algorithm at 75 (A), 85 (B) and 110 m (C), orthomosaics of Cockroach Caye were classified by the RT algorithm at 75 m (D), 85 m (E) and 110 m (F).

Figure A5. Average percentage cover (%) of classified coral, sand (\pm SE), sea (\pm SE), seagrass (\pm SE), and mangrove at the survey altitudes of 75 m, 85 m and 110 m, with 95% confidence interval.